take place between itself and three novobiocin molecules. Fig. 2 shows that two of these are related by the twofold screw axis along x (effectively holding opposite ends of the molecules together), the remaining hydrogen bonds are to O(1) and O(2) on a symmetry related sugar ring, resulting in a continuous linkage of the sugar rings in the y direction by hydrogen bonds.

There is possibly further intermolecular hydrogen bonding between O(5) and the carbamyl nitrogen N(1) on adjacent molecules (Fig. 3), the separation of these atoms being 3·083 Å. Thus the sugar rings of adjacent molecules are linked in the x direction. The hydrogen-bond distances involved between the donor and acceptor atoms are shown in Table 6. The distance of 4·481 Å between N(1) and the enolic oxygen O(7) on the coumarin system eliminates the possibility of interaction between these groups (Brock, 1967).

Table 6. *Distances and their standard deviations* (Å) *between donor and acceptor atoms involved in hydrogen bonding*

Donor	Acceptor	Type of bond	
O(4)	O(12)	OH $\cdots H_2O$	2·814 (14)
O(12)	O(2)	$H_2O\cdots C{=}O$	2·712 (15)
O(12)	O(1)	$H_2O\cdots$–O–	2·854 (14)
O(11)	O(12)	OH $\cdots H_2O$	2·771 (14)
O(7)	O(10)	OH $\cdots C{=}O$	2·446 (12)
N(1)	O(5)	NH $\cdots$–O–	3·075 (15)

At this stage it would seem highly desirable to recrystallize the novobiocin again in an attempt to produce crystals suitable for more accurate data collection and possibly to eliminate the presence of Ca^{2+} ions. This work is in progress and further discussion of the structure will be published later.

The authors wish to acknowledge and thank the Governors of Plymouth Polytechnic for permission to carry out this work, the Medical Research Council for a grant, the Boots Pure Drug Company for their generous supply of the starting material and the Science Research Council Computer Centre for the allocation of computer facilities. We thank also Mr A. E. Bird for obtaining the n.m.r. spectra and Dr S. Shall and Mr R. J. Girven for advice concerning crystallization and discussion of the results.

References

Brock, T. D. (1967). *Antibiotics*, **1**, 651–665.

Germain, G., Main, P. & Woolfson, M. M. (1971). *Acta Cryst.* A**27**, 368.

Golding, B. T. & Rickards, R. W. (1963). *Chem. Ind.* pp. 1081–1083.

Hauptman, H. & Karle, J. (1953). *Solution of the Phase Problem.* 1. *The Centrosymmetric Crystal.* ACA Monograph No. 3. Pittsburgh: Polycrystal Book Service.

Hauptman, H. & Karle, J. (1956). *Acta Cryst.* **9**, 45–55.

Hoeksema, H. & Smith, C. G. (1961). *Prog. Ind. Microbiol.* **3**, 91–139.

International Tables for X-ray Crystallography (1962). Vol. III, p. 202. Birmingham: Kynoch Press.

Karle, J. & Hauptman, H. (1956). *Acta Cryst.* **9**, 635–651.

Morris, A. & Russell, A. D. (1971). *Prog. Med. Chem.* **8**, 39–59.

Acta Cryst. (1975). B**31**, 1406

The Crystal Structure of $Y_7O_6F_9$

By D. J. M. Bevan and A. W. Mann*

The Flinders University of South Australia, Bedford Park, South Australia, 5042

(*Received* 11 *October* 1974; *accepted* 23 *December* 1974)

The compound $Y_7O_6F_9$ is an anion-excess, fluorite-related phase, which is a basic structural unit in a series of intergrowth phases in the Y_2O_3–YF_3 system. It crystallizes in the space group *Abm*2 with orthorhombic cell dimensions $a=5{\cdot}420\pm0{\cdot}001$, $b=38{\cdot}58\pm0{\cdot}01$, $c=5{\cdot}527\pm0{\cdot}001$ Å and four formula units per unit cell. Despite the presence of 'inverse overlap' the structure of $Y_7O_6F_9$ has been solved and the unit cell shown to contain two regions of almost undistorted structure types, fluorite and YF_3-type, between which a gradual and coherent change in structure type occurs. $Y_7O_6F_9$ is an important structure in the development of the 'vernier concept' for intergrowth phases in the Y_2O_3–YF_3 system.

Introduction

The composition region $YX_{2.13}$–$YX_{2.22}$ ($X=O+F$) of the Y_2O_3–YF_3 system contains an apparently infinite number of long-period fluorite-related superstructure phases which are based on one-dimensional ordered intergrowth of several simpler 'basic unit orthorhombic phases' (Mann & Bevan, 1972). These 'basic unit orthorhombic phases' are members $n=4,5,6,7,8$ of the homologous series $Y_nO_{n-1}F_{n+2}$, and have unit cells with dimensions a,nb,c, where a, b, and c are dimen-

---

* Present address: CSIRO, Division of Mineralogy, Private Bag, P.O., Wembley, Western Australia, 6014.

sions of the fluorite subcell. The unit cells consist, in essence, of n fluorite-type subcells stacked one upon the other in the **b** direction, two of which accommodate the anions in excess of the fluorite complement. This paper describes the crystal structure of member $n=7$ of this series, the phase $Y_7O_6F_9$, which occurs within the orthorhombic phases region $YX_{2.13}$–$YX_{2.22}$ at the (ideal) composition $YX_{2.143}$.

Experimental

Single crystals for the structure determination were selected from the diphasic mixture resulting from heating a powdered mixture of Y_2O_3 (99·99 %) and YF_3 (99·9 %) in a sealed platinum capsule for several days at temperatures up to 1200 °C. One crystal, with approximate dimensions $0{\cdot}12\times0{\cdot}10\times0{\cdot}06$ mm was chosen for an initial structure determination with visually estimated intensity data. Subsequently a second crystal, approximately spherical and 0·11 mm in diameter, was chosen for structure refinement using data collected on a diffractometer.

Systematic absences were obtained from preliminary Weissenberg and precession photographs, and lattice parameters were obtained with a Hägg–Guinier focusing camera using monochromatic Cu $K\alpha_1$ radiation. The crystal data are shown in Table 1.

Table 1. *Crystal data for* $Y_7O_6F_9$

Formula	$Y_7O_6F_9$
Crystal system	Orthorhombic
Cell dimensions	$a=5{\cdot}420\pm0{\cdot}001$ Å $b=38{\cdot}58\pm0{\cdot}01$ $c=5{\cdot}527\pm0{\cdot}001$
Systematic absences	hkl when $k+l=2n+1$ $0kl$ when $k=2n+1$
D_m (pycnometric)	5·09 g cm^{-3}
D_c	5·11 g cm^{-3}
Z	4
μ(Cu $K\alpha$)	501·8 cm^{-1}
Space groups	*Abm*2 (No. 39), *Cmma* (No. 67)

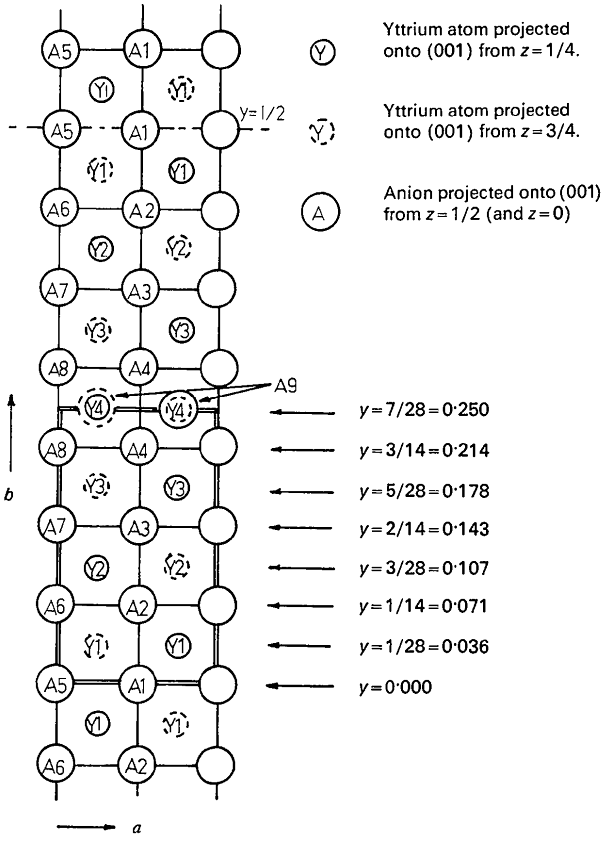

Fig. 1. Idealized structure for $Y_7O_6F_9$ projected onto (001). The asymmetric unit is shown in double outline.

Integrated Weissenberg intensity data were recorded with Cu $K\alpha$ radiation for the first five layers along [100] using the multiple-film technique. Intensities for reflexions with h,k,l positive were estimated by visual comparison with a standard intensity strip containing spots of a similar size and shape to the integrated reflexions. Lorentz, polarization and absorption corrections were applied to the 387 measured reflexions.

Diffractometer data were collected, again using Cu $K\alpha$ radiation, on a two-circle computer-controlled equi-inclination X-ray diffractometer, similar to that described by Freeman, Guss, Nockolds, Page & Webster (1970). Intensities for reflexions with h,k,l positive and with $15° < \tau < 140°$ were measured from the first six layers along [100] and the first six layers along [001] of the same crystal. The scan speed, dependent on the intensity of the reflexion, varied between 0·02° s^{-1} and 0·33° s^{-1} and the scan range, $\Delta\varphi$, varied from 1·5 to 3·0°. A total of 581 independent reflexions were measured; of these 349 were assigned as 'observed' based on an intensity $I > 2{\cdot}1\sigma(I)$, where $\sigma(I)$ is the statistical standard deviation for the measurement. Lorentz, polarization and absorption (spherical) corrections were subsequently applied to the data.

Structure determination and refinement

Patterson function

A Patterson synthesis was performed on the visually estimated intensity data to verify the assumed relationship of the structure to a fluorite-based stacking sequence. This assumption was overwhelmingly confirmed; very little but the fluorite-type vectors could be recognized in Patterson projections. This was apparently due to the sevenfold fluorite repeat nature of the cell, and in particular to the similarities between positions of yttrium atoms within each subcell. Due to the large differences in scattering factors between yttrium and oxygen and fluorine, very little information about anion displacements from ideal fluorite positions, or the location of the interstitial anion, could be obtained from the Patterson synthesis.

Choice of space group and setting

The eightfold general set of space group *Abm*2 generates the following set of equivalent positions:

$$x,y,z;\ \bar{x},\bar{y},z;\ \bar{x},\tfrac{1}{2}+y,z;\ x,\tfrac{1}{2}-y,z;$$
$$x,y+\tfrac{1}{2},z+\tfrac{1}{2};\ \bar{x},\tfrac{1}{2}-y,\tfrac{1}{2}+z;\ \bar{x},y,\tfrac{1}{2}+z;\ x,\bar{y},\tfrac{1}{2}+z\ .$$

Inspection of the structure factor (F_o) lists, in particular of reflexions with any two indices identical, indicated that shifts in all three positional parameters for some if not all atoms were required. The fourfold sets, 4(*a*), 4(*b*), 4(*c*) of *Abm*2 and the eight and fourfold sets of *Cmma* do not allow for change in all three positional parameters. With this condition imposed, a sevenfold fluorite-type stacking sequence can only be arranged in *Abm*2 with the long crystallographic axis of the unit cell consistent with the *b* axis of the space group. The idealized model for the structure, a stack of seven fluorite-type subcells, is built up by placing atoms in the following positions.

Yttrium atoms: Y(1), Y(3) into 8(*d*): $x=\frac{3}{4}, y=\frac{1}{28}, \frac{5}{28}, z=\frac{1}{4}$; Y(2) into 8(*d*): $x=\frac{1}{4}, y=\frac{3}{28}$, $z=\frac{1}{4}$; Y(4) into 4(*c*): $x=\frac{1}{4}, y=\frac{1}{4}, z=\frac{1}{4}$.

Anions (A = oxygen or fluorine): A(2), A(3), A(4), into 8(*d*): $x=\frac{1}{2}, y=\frac{1}{14}, \frac{2}{14}, \frac{3}{14}$, $z=0$; A(6), A(7), A(8) into 8(*d*): $x=0, y=\frac{1}{14}, \frac{2}{14}, \frac{3}{14}, z=0$; A(1) into 4(*b*): $x=\frac{1}{2}, y=0, z=0$; A(5) into 4(*a*): $x=0, y=0$, $z=0$.

Interstitial: A(9) into 4(*c*): $x, y=\frac{1}{4}, z$ (if $\frac{1}{2}<x<1$ and $0<z<\frac{1}{2}$ the interstitial will be in a 'vacant' fluorite-type anion cube).

The idealized structure for $Y_7O_6F_9$ is shown in Fig. 1.

Refinement of the idealized structure

Katz & Megaw (1967) outline the problems and dangers associated with refinement from an idealized structure of higher symmetry; in the present case direct refinement of the idealized model proved unsatisfactory. In addition, the close relationship to fluorite proved an early barrier to the determination of positions for anions A(5), A(6), A(7), A(8) and A(9). Peaks for anions A(1), A(2), A(3) and A(4) were clearly evident in difference (F_o-F_c) Fourier maps calculated with yttriums in their fluorite-type sites, but peaks at or near the sites $x=0, y=\frac{1}{14}, \frac{2}{14}, \frac{3}{14}, z=0$ were poorly defined and mirrored across the $z=\frac{1}{4}$ (metal containing) plane. Attempts to refine models with yttrium and some anion positions included, all of which produced significant improvements in the residual R $(=\sum|F_o-F_c|/\sum|F_o|)$ from 0·50 to around 0·22, resulted in high errors in *z* parameter shifts for metal atoms and high correlations between some parameters. These features are symptomatic of the problem of 'inverse overlap' described by Geller (1961), Srinivasan (1961), Rae & Maslen (1963) and Evans (1961), and in the present case due to the existence of an arbitrary positional parameter (*z*) perpendicular to a centrosymmetric projection.

These initial refinements showed, espited the presence of inverse overlap, that regardless of positions chosen for anions A(5), A(6), A(7), A(8) and A(9), shifts in the *x* parameters for yttrium atoms were always towards the anions A(1), A(2), A(3) and A(4), parameter shifts in *y* from the ideal model were always small, and directions and magnitudes of *z*-parameter shifts from the ideal sites were influenced markedly by the choice of positions for anions in the structure. Positions for the yttrium atoms in the structure were finally established by refinement with only anions A(1), A(2), A(3) and A(4) in position, and with initial *x* and *y* parameter values for yttriums consistent with the above observations.

The difference Fourier synthesis taken after this refinement, in contrast to earlier maps, contained only five distinct additional anion-type peaks; Fig. 2 shows the projections from layers $z=\frac{3}{20}$ and $x=\frac{7}{20}$ of this difference Fourier superimposed on the (001) plane.

Refinement of the structure

Refinement of the visually estimated data, with yttrium and anion positions obtained from the difference Fourier maps, ultimately produced a value for R of 0·150. The more accurately measured intensity data from the diffractometer subsequently became available, and refinement of atom positions and thermal parameters was continued with these data. Least-squares refinements were carried out using a modification of the full-matrix least-squares program *ORFLS* (Busing, Martin & Levy, 1962). The function minimized was $\sum w(F_o-F_c)^2$, with w the weight for each reflexion inversely proportional to the variance in the measured structure factor. Using ionic scattering factors for all atoms, given by Cromer & Waber (1965), and with

Table 2. *Anion models for* $Y_7O_6F_9$ *and their R values*

Model No. (m)	A(2)	A(3)	A(6)	A(7)	R_m	R_m/R_3	$\mathscr{R}$(Hamilton)
1	F	O	F	O	0·086	1·029	1·019
2	O	F	O	F	0·087	1·037	1·019
3	O	O	F	F	0·084	1·000	
4	F	F	O	O	0·091	1·083	1·027
5	O	F	F	O	0·086	1·022	1·019
6	F	O	O	F	0·086	1·022	1·019

Table 3. *Atomic positions and thermal parameters for* $Y_7O_6F_9$

The form of the anisotropic temperature factors is $\exp[-(\beta_{11}h^2+\beta_{22}k^2+\beta_{33}l^2+2\beta_{12}hk+2\beta_{13}hl+2\beta_{23}kl)]$. The β are $\times 10^4$. The number in parentheses is the standard deviation and refers to the least significant digits.

	x	y	z	β_{11}	β_{22}	β_{33}	β_{12}	β_{13}	β_{23}
Y(1)	0·714 (2)	0·0359 (2)	0·250	183 (38)	2·9 (3)	200 (40)	−2·5 (48)	48 (42)	5·4 (20)
Y(2)	0·295 (2)	0·1076 (2)	0·286 (2)	163 (44)	1·9 (4)	49 (34)	1·0 (40)	−39 (44)	2·0 (27)
Y(3)	0·715 (2)	0·1798 (2)	0·243 (3)	190 (52)	2·6 (4)	203 (48)	−3·1 (43)	34 (25)	5·1 (27)
Y(4)	0·294 (4)	0·250	0·294 (3)	193 (70)	1·8 (5)	13 (38)	0	0	0

Table 3 (*cont.*)

	x	y	z	B
O(1)	0·500	0·000	0·478 (18)	1·53 (92)
O(2)	0·489 (20)	0·0723 (14)	0·019 (13)	2·28 (121)
O(3)	0·468 (15)	0·1436 (11)	0·996 (9)	0·80 (110)
F(4)	0·442 (11)	0·2132 (14)	0·010 (13)	2·72 (98)
O(5)	0·000	0·0000	0·057 (16)	1·33 (86)
F(6)	0·031 (14)	0·0631 (10)	0·400 (10)	2·43 (103)
F(7)	0·940 (14)	0·1273 (12)	0·121 (12)	2·08 (96)
F(8)	0·103 (11)	0·1913 (11)	0·369 (10)	1·95 (89)
F(9)	0·920 (15)	0·2500	0·122 (13)	2·13 (91)

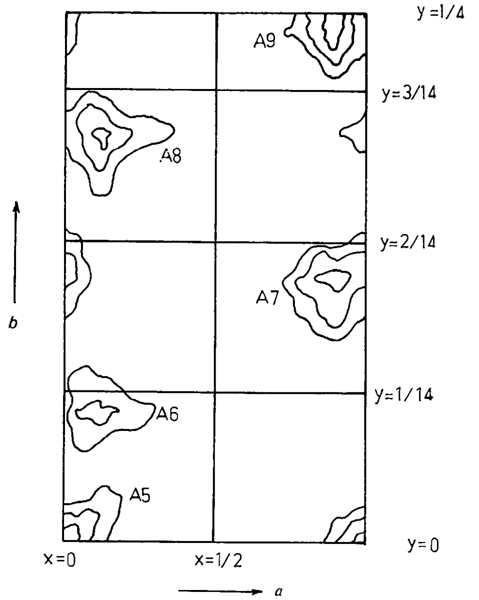

Fig. 2. Projections onto (001) from sections $z=\frac{3}{20}$, $z=\frac{7}{20}$ of a difference Fourier map taken with yttrium atoms in non-ideal sites and with anions A(1), A(2), A(3) and A(4) included. The contours are drawn at equal intervals on an arbitrary scale.

$f_{O^{2-}}=f_{F^-}$, the value for the residual R, after refining positional parameters for all atoms and anisotropic thermal parameters for yttriums, was 0·099.

In order to simplify the determination of the correct distribution of 24 oxygens and 36 fluorines over the 6×8-fold and 3×4-fold sets available, two criteria to reduce the number of possibilities were applied. Firstly, anions A(4), A(8) and A(9) were in all cases chosen as fluorines; the coordination of Y(4), which involves these anions, was noted at this stage to be almost identical to the coordination of Y in YF_3 (this is pointed out in detail in the Discussion). Secondly, anions A(1) and A(5) in the sets 4(*a*), 4(*b*) were selected as oxygens; initial attempts to refine with fluorines in these sites led to very high positive thermal parameters for these atoms. The six distinct models which result from distributing the remaining 16 oxygens and 16 fluorines over the eightfold sites of A(2), A(3), A(6) and A(7) are shown in Table 2.

A refinement of positional parameters for all atoms, anisotropic thermal parameters for yttriums, and with atomic scattering factors for yttriums, oxygens and fluorines (Cromer & Waber, 1965) included, was performed for each of the six anion distributions. The final values for parameters were the same, within the e.s.d.'s, for each model; differences in the values of the residual, R, were however evident. As a final test for the significance of the different oxygen and fluorine distributions, a residual, R_m, was calculated for each model (m) using an identical set of atom parameters and with the distribution of oxygen and fluorine scattering factors as the only difference between each calculation. The values for the residuals, R_m, are shown in Table 2. The value for R_3 is the lowest (*N.B.* the other values are higher than this by amounts apparently dependent on whether the model has two or four scattering factors different from model 3). Ratios

Table 4. *Observed and calculated structure factors*

The columns in each group list k, $10F_o$, $10F_c$, and 100σ (F_o). The asterisks denote reflexions treated as unobserved.

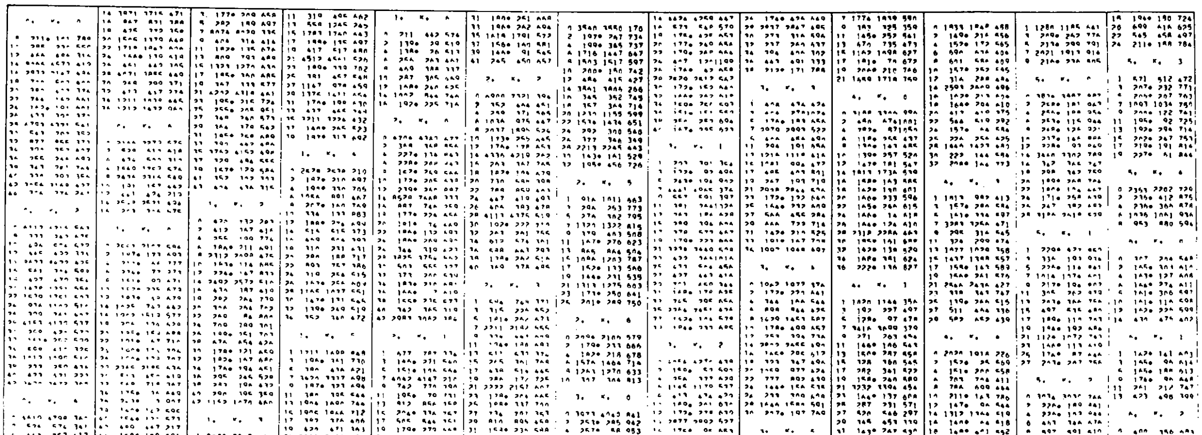

R_m/R_3 of observed residuals for all models compared to the best model, R_3, are shown in Table 2. In all cases this ratio is greater than the corresponding value of $\mathscr{R}$ from the Hamilton $\mathscr{R}$ test (Hamilton, 1965), calculated for the appropriate number of parameters changed and degrees of freedom present, at the $\frac{1}{2}$% significance level. The anion arrangement of model 3 thus produces an improvement in the residual R which at this level of confidence and according to this test is a statistically significant one.

Oxygen and fluorine scattering factors according to the distribution in model 3 were used in a final refinement of the structure. Isotropic temperature factors for the anions were refined in the final cycle along with all positional parameters, scale and extinction parameters and anisotropic thermal parameters for yttrium atoms. The final value for the residual R was 0·076. Of the 64 parameters refined, eight pairs had final correlations in excess of 0·50. In all but two cases the high correlations were between z or β_{33} parameters of adjacent atoms; the two exceptions were for the correlations between x Y(1) and x Y(2), and x F(6) and x F(7). The final positional and thermal parameter values are shown in Table 3; the high standard deviations are due to inverse overlap.

The observed and calculated structure factors obtained with these parameters are given in Table 4.

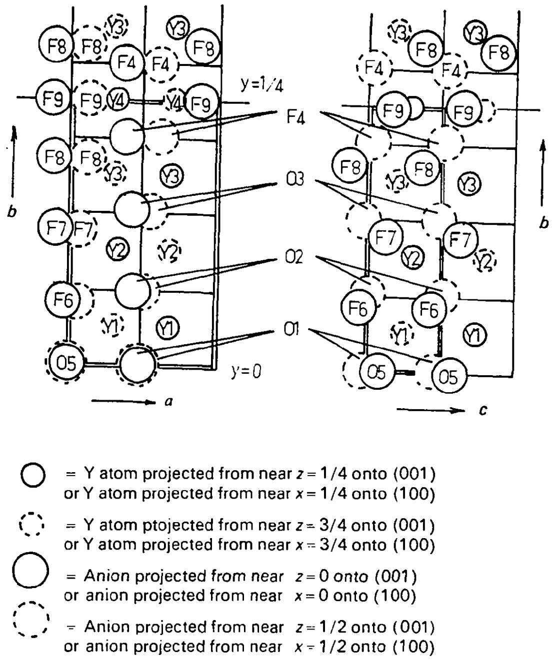

Fig. 3. Projections of the crystal structure of $Y_7O_6F_9$ onto (001) and (100). The asymmetric unit is shown in double outline.

Discussion

Two projections of the final $Y_7O_6F_9$ structure, with oxygens and fluorines distinguished, are shown in Fig. 3.

Differences between refined and ideal structures

The following differences between the refined and the ideal structures (*i.e.* the deviations from ideal fluorite) are evident.

(*a*) y parameter values for the row of anions O(1), O(2), O(3), F(4) are close to the initial (fluorite) values. y parameter values for the row of anions O(5), F(6), F(7), F(8), F(9), which contains one more anion than the equivalent fluorite-type row, are significantly different from initial (fluorite) values but very close to the values one obtains by distributing five anions (four spaces) evenly over the length of the asymmetric unit (*i.e.* $n/4\times0{\cdot}250=0{\cdot}000$, 0·062, 0·126, 0·188 and 0·250, where n = integer 0, 1, 2, 3 or 4).

(*b*) Anion pairs with similar y parameter values, *i.e.* pairs O(1)–O(5), O(2)–F(6), O(3)–F(7), F(4)–F(8), are 'staggered' in z relative to the adjacent anion pairs (see Fig. 3).

(*c*) Anion F(9), the 'interstitial', is significantly removed from the classical fluorite interstitial site $\frac{1}{2},\frac{1}{2},\frac{1}{2}$ in a face-centred cube ($\frac{3}{4},\frac{1}{4},\frac{1}{4}$ in the present cell).

Coordination of Y(1), Y(2), Y(3) *and* Y(4)

Yttrium–anion interatomic distances are shown in Table 5.

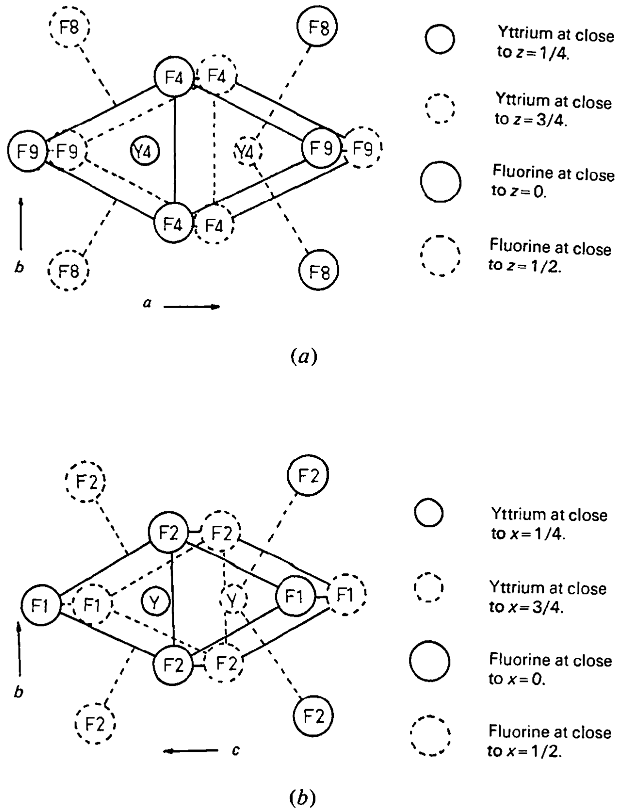

Fig. 4. (*a*) Projection of the $Y_7O_6F_9$ structure near Y(4) atoms onto (001). (*b*) Projection of part of the YF_3 structure onto (100) on the same scale.

Table 5. *Yttrium–anion interatomic distances in* $Y_7O_6F_9$ (Å)

Y(1)–F(6)	2·18 (7)	Y(2)–O(2)	2·21 (8)
Y(1)–O(1)	2·20 (6)	Y(2)–O(3)	2·22 (6)
Y(1)–O(2)	2·26 (8)	Y(2)–F(7)	2·26 (7)
Y(1)–O(2)	2·33 (8)	Y(2)–O(2)	2·27 (7)
Y(1)–O(5)	2·33 (4)	Y(2)–O(3)	2·32 (6)
Y(1)–O(1)	2·35 (6)	Y(2)–F(6)	2·33 (6)
Y(1)–F(6)	2·60 (6)	Y(2)–F(7)	2·37 (7)
Y(1)–O(5)	2·68 (6)	Y(2)–F(6)	3·26 (5)
Y(3)–F(4)	2·13 (7)	Y(2)–F(8)	3·42 (5)
Y(3)–O(3)	2·21 (6)	Y(4)–F(9)	2·15 (7)
Y(3)–F(8)	2·26 (6)	Y(4)–F(9)	2·24 (8)
Y(3)–F(8)	2·33 (6)	Y(4)–F(4)	2·26 (7)
Y(3)–F(4)	2·35 (6)	Y(4)–F(4)	2·26 (7)
Y(3)–O(3)	2·37 (6)	Y(4)–F(4)	2·34 (6)
Y(3)–F(7)	2·46 (5)	Y(4)–F(4)	2·34 (6)
Y(3)–F(9)	3·00 (4)	Y(4)–F(8)	2·52 (5)
Y(3)–F(7)	3·45 (7)	Y(4)–F(8)	2·52 (5)
		Y(4)–F(9)	3·53 (8)

All interatomic distances less than 4 Å were initially calculated; it was clear that each yttrium had either seven or eight anions within 2·7 Å and all others at distances greater than 3·0 Å. The nearest-neighbour coordination numbers on this basis are: C.N. [Y(1)]= 8. C.N. [Y(2)]=7, C.N.[Y(3)]=7, C.N.[Y(4)]=8. However, all metals except Y(1) have additional anions between 3·00 Å and 3·60 Å; the interatomic distances for these are included in Table 5. The coordination number of yttrium in YF_3 is described as 8(+1) (Zalkin & Templeton, 1953); in the present structure the anion arrangements about each yttrium are distinctly more distorted from the fluorite-type anion cube in the order Y(4) > Y(3) > Y(2) > Y(1). If projections of the $Y_7O_6F_9$ structure [from near Y(4)] and the YF_3 structure are compared (see Fig. 4), the coordination environment for Y(4) is seen to be almost identical to that for Y in YF_3.

In the YF_3 structure, six of the anions surrounding each Y are arranged at the apices of a trigonal prism, with an additional anion beyond each of the lateral faces. The eight closely coordinated anions about Y(4) in the present structure are disposed in a similar, though slightly distorted manner. A ninth anion beyond the remaining lateral face of the trigonal prism is at a somewhat greater distance (3·53 Å) than in YF_3. The anion arrangement around Y(3) has a similar, though even more distorted relationship to that around Y in YF_3.

These similarities suggest that the structure of $Y_7O_6F_9$, which occurs as a phase with composition intermediate between YOF (which has a slightly distorted fluorite-type structure) and YF_3, may be regarded as an intermediate phase in which characteristics of the 'parents' appear at the unit-cell level. The structure of $Y_7O_6F_9$, formally, is one which contains regions of two almost undistorted structure-types, fluorite-type around Y(1) and YF_3-type around Y(4), between which a gradual and coherent transition in structure type occurs.

On the basis of this structure for $Y_7O_6F_9$, Hyde, Bagshaw, Andersson & O'Keeffe (1974) have developed the elegant concept of 'vernier' structures, which enables a simple structural description to be given for all of the much larger superlattice phases in the composition range $YX_{2\cdot13}$–$YX_{2\cdot22}$ described in a previous publication (Mann & Bevan, 1972). Since the present work was completed Jung & Juza (1973) have published the structure of a complex zirconium nitride fluoride, the basic structural features of which are similar to those of $Y_7O_6F_9$. Their calculations are based on a cell 1 × 27 × 1 fluorite units along **a**, **b** and **c** respectively, and confirm the 'vernier' description for superlattice phases.

References

Busing, W. R., Martin, K. O. & Levy, H. A. (1962). *ORFLS*. Oak Ridge National Laboratory Report ORNL-TM-305.

Cromer, D. T. & Waber, J. T. (1965). *Acta Cryst.* **18**, 104–111.

Evans, H. T. (1961). *Acta Cryst.* **14**, 1019–1026.

Freeman, H. C., Guss, J. M., Nockolds, C. E., Page, R. & Webster, A. (1970). *Acta Cryst.* A**26**, 149–152.

Geller, S. (1961). *Acta Cryst.* **14**, 1026–1035.

Hamilton, W. C. (1965). *Acta Cryst.* **18**, 502–510.

Hyde, B. G., Bagshaw, A. N., Andersson, S. & O'Keeffe, M. (1974). *Ann. Rev. Mater. Sci.* **4**, 43–92.

Jung, W. & Juza, R. (1973). *Z. anorg. allgem. Chem.* **399**, 129–147.

Katz, L. & Megaw, H. D. (1967). *Acta Cryst.* **22**, 639–648.

Mann, A. W. & Bevan, D. J. M. (1972). *J. Solid State Chem.* **5**, 410–418.

Rae, A. I. M. & Maslen, E. N. (1963). *Acta Cryst.* **16**, 703–704.

Srinivasan, R. (1961). *Acta Cryst.* **14**, 1163–1167.

Zalkin, A. & Templeton, D. H. (1953). *J. Amer. Chem. Soc.* **75**, 2453–2458.